AIAA JOURNAL
Vol. 45, No. 9, September 2007

Technical Notes

TECHNICAL NOTES are short manuscripts describing new developments or important results of a preliminary nature. These Notes should not exceed 2500 words (where a figure or table counts as 200 words). Following informal review by the Editors, they may be published within a few months of the date of receipt. Style requirements are the same as for regular contributions (see inside back cover).

Computation of Radiation in the Apollo AS-501 Reentry Using Opacity Distribution Functions

A. A. Wray
NASA Ames Research Center, Moffett Field, California 94035
J.-F. Ripoll
Los Alamos National Laboratory, Los Alamos, New Mexico 87544
and
D. Prabhu
ELORET Corporation, Sunnyvale, California 94086

DOI: 10.2514/1.28520

I. Introduction

FOR calculating radiation in reentry problems, the variation of the radiation with frequency must be addressed. Complex frequency dependence appears in both the source function and the opacity (or absorption coefficient, cm^{-1}) field of the radiative transfer equation (RTE). This complexity is due to a very large number of bound–bound and bound–free transitions happening in very hot, partially ionized, nonequilibrium air. Full resolution of the problem is possible but requires treatment of the radiation transport at $\sim 10^7$ frequencies. Such computations are commonly done at NASA Ames Research Center using the NEQAIR96 code [1] to postprocess flowfield data. This fully resolved approach is infeasible in a time-dependent computation due to extreme computational cost. There are many methods to reduce the cost of the solution, and we can divide these into two families [2]. One can divide the frequency spectrum into n_g contiguous groups, average, and solve the transport for each group; these are the multigroup methods. Or one can reorganize the frequency spectra into n_b opacity bins or pickets, according to the value of the opacity [2]. This creates disjointed sets of frequencies ν, the bins or pickets, with similar mean opacities. The second method is usually referenced as the *opacity distribution function* (ODF) method and as been in use for many years [2–6]. It is based on the key recognition that *transport depends on the value of the opacity, not the value of the frequency*, as stated in [7]. In its usual and sophisticated form, the ODF method, also called the multiband method [8], merges both approaches by reorganizing the opacity into n_b bins inside each of the n_g groups.

In our case, we compare the results of 1) the multiband technique in which $n_g = n$ groups are defined but with a single bin $n_b = 1$ inside each group (this is simply the multigroup approach), versus 2) the multiband technique in which a single group is defined for the whole spectrum ($n_g = 1$) but which is divided into $n_b = n$ bins. For simplicity and clarity, we designate this as the multibin method. The multibin method has notably been used by astrophysicists for solar computations [5,9]. The goal of this paper is to compare the multigroup and multibin methods for the Apollo AS-501 reentry. We demonstrate that it allows solution of this reentry radiation problem with high accuracy for a very low number of bins (10 bins), an accuracy that is attained by the multigroup approach for only a very large number of groups.

II. Binning Algorithm and Equations

To define our notation, we write the time-independent radiative transfer equation for direction $\mathbf{\Omega}$, source $S(\nu, \mathbf{x})$, opacity $\sigma(\nu, \mathbf{x})$, and intensity $I(\nu, \mathbf{x})$ as follows:

$$\mathbf{\Omega} \cdot \nabla_{\mathbf{x}} I(\nu, \mathbf{x}) = \sigma(\nu, \mathbf{x})[S(\nu, \mathbf{x}) - I(\nu, \mathbf{x})] \tag{1}$$

We have suppressed the dependence of I on $\mathbf{\Omega}$ for simplicity of notation, and $\mathbf{x}$ denotes all spatial coordinates. To create the bins in ν space, we first define an $\mathbf{x}$-independent mean opacity $\langle\sigma\rangle(\nu)$, which is formed by weighting with the source as follows:

$$\langle\sigma\rangle(\nu) = \frac{\int_{\mathbf{x}} S(\nu, \mathbf{x})\sigma(\nu, \mathbf{x})\, \mathrm{d}^3 x}{\int_{\mathbf{x}} S(\nu, \mathbf{x})\, \mathrm{d}^3 x} \tag{2}$$

The bins are defined using a mean opacity so as to be the same for all spatial points. The set of frequencies in bin i is defined to be $\{\nu_i\} = \{\nu | \langle\sigma\rangle(\nu) \in [\sigma_{i-\frac{1}{2}}, \sigma_{i+\frac{1}{2}})\}$. The dividing values $\sigma_{i-\frac{1}{2}}, \sigma_{i+\frac{1}{2}}$ are chosen to be equally spaced logarithmically (i.e., $\sigma_{i-\frac{1}{2}}/\sigma_{i+\frac{1}{2}} = \mathrm{const}$ for all i). Next, we integrate the RTE (1) over each bin i. This leads to an unclosed term:

$$\int_{b(\nu)=i} \sigma(\nu, \mathbf{x}) I(\nu, \mathbf{x})\, \mathrm{d}\nu$$

where we have written $b(\nu) = i$ if frequency ν is in bin i; that is, if $\langle\sigma\rangle(\nu) \in [\sigma_{i-\frac{1}{2}}, \sigma_{i+\frac{1}{2}})$. We approximate the unclosed term by defining a mean opacity over the ith bin, $\bar{\sigma}_i(\mathbf{x})$, in a source-weighted manner:

$$\bar{\sigma}_i(\mathbf{x}) = \frac{\int_{b(\nu)=i} S(\nu, \mathbf{x})\sigma(\nu, \mathbf{x})\, \mathrm{d}\nu}{\int_{b(\nu)=i} S(\nu, \mathbf{x})\, \mathrm{d}\nu} \tag{3}$$

If the source $S(\nu, \mathbf{x})$ were Planckian, which it is not in the Apollo case, Eq. (3) would be the Planck mean opacity in a bin [2]. The unclosed term is approximated as

$$\int_{b(\nu)=i} \sigma(\nu, \mathbf{x}) I(\nu, \mathbf{x})\, \mathrm{d}\nu \approx \bar{\sigma}_i(\mathbf{x}) \int_{b(\nu)=i} I(\nu, \mathbf{x})\, \mathrm{d}\nu \tag{4}$$

Mean opacities other than Eqs. (2) and (3) could, of course, be used to define the bins and to approximate the unclosed term in the bin-integrated RTE [10]. Two obvious possibilities are the simple arithmetic (unweighted) and the Rosseland means. We experimented with these two means using artificially generated source and opacity functions and, for the unweighted mean opacity, using the Apollo data as well. In nearly all instances, the source-weighted form gives more accurate results, though there are some cases in which the

Received 24 October 2006; revision received 12 May 2007; accepted for publication 20 May 2007.

unweighted form is slightly more accurate, but this is outweighed by other instances in which this mean is much less accurate than the source-weighted mean. The total source function in bin i, S_i, is simply

$$S_i(\mathbf{x}) = \int_{b(\nu)=i} S(\nu, \mathbf{x})\, \mathrm{d}\nu$$

We can now write the RTE for each bin i as

$$\boldsymbol{\Omega} \cdot \nabla_{\mathbf{x}} I_i(\mathbf{x}) = \bar{\sigma}_i(\mathbf{x})[S_i(\mathbf{x}) - I_i(\mathbf{x})] \tag{5}$$

where I_i is the total intensity in bin i:

$$\int_{b(\nu)=i} I(\nu, \mathbf{x})\, \mathrm{d}\nu$$

The only approximation is Eq. (4). Because the binning is not $\mathbf{x}$-dependent, the spatial derivative operator commutes with the binning operation. The final step is to discretize ν space. For the Apollo data, the already discretized set of frequencies $\{\nu_j\}$ is simply divided into bins as done previously to form a subset $\{\nu_{i_k}\}$ for each bin:

$$i\colon \{\nu_{i_k}, k = 1, \ldots, k_{\max}\} = \{\nu_j | \langle\sigma\rangle(\nu_j) \in [\sigma_{i-\frac{1}{2}}, \sigma_{i+\frac{1}{2}})\}$$

In general, the number of frequency samples per bin, $k_{\max}$, vary from bin to bin. In the multigroup case, the same steps are followed, but the quantities are integrated over contiguous ν subsets of equal size; that is, the grouping method chosen is simply to divide all of ν space into equal-sized groups. It may not be an optimal choice of groups.

III. Apollo AS-501 Reentry Data

The AS-501 flight was chosen because its flight trajectory was, by design, very similar to those of spacecraft returning from the moon and hence generated the highly nonequilibrium shock layer that will be present in future crew exploration vehicle reentries from the moon and Mars. The specific conditions present at the point in the trajectory at which the simulations were made are altitude 58.84 km, velocity 10.15 km/s, freestream temperature 267 K, density 3.94×10^{-4} kg/m^3, and vehicle attitude 24.9 deg. The radiation field of the Apollo AS-501 reentry has been simulated using data from the NEQAIR96 code [1]. NEQAIR has been largely used at NASA Ames Research Center and is, for instance, well described and referenced in [11]. NEQAIR96 was used to generate the source and opacity as functions of space for 1.09×10^7 frequencies and also to compute the radiative intensity along a line leading from the shock layer to the stagnation point of the vehicle. The source and opacity were calculated from the following quantities: kinetic, electron, rotational, and vibrational temperatures, and species concentrations of the nonequilibrium air plasma. Such a detailed aerothermodynamic data set cannot be obtained from measurements, because it requires a large number of physical quantities at high spatial and temporal resolution. The aerothermodynamic quantities needed by NEQAIR96 were obtained from simulations with the data parallel line relaxation (DPLR) code [12] of NASA Ames Research Center and validated against existing measurements ([13] describes the codes and methods used for the Apollo reentry for flight AS-202, but exactly the same techniques and validations were applied in the case of AS-501). In Fig. 1, we plot the source function at the shock (left) and at the nose of the vehicle (right). Similarly, the opacity is shown in Fig. 2. Both profiles attest to the complexity of the problem.

IV. Numerical Results

We first compare two computations of the radiative intensity, one with 100 frequency groups and one with 100 bins ($n_g = n_b = 100$). The results are shown in Fig. 3 (left), along with the exact solution (i.e., the intensity computed as the sum over all 1.09×10^7 frequencies of the data set, each separately transported). The solution obtained with 100 bins is very close to the exact solution, whereas the multigroup solution is off by factors up to 15. Two coarser computations were done using 10 groups and 10 bins, and these results are compared with the exact solution in Fig. 3 (right). The multigroup solution is off by factors of 10 to 20, and little improvement occurs in going from 10 groups to 100. This implies that a much larger number of groups is likely to be needed to reach good accuracy, a conclusion verified next. On the other hand, the 10-bin solution is already very close to the exact one and to the solution obtained with 100 bins. This confirms that only a few bins are needed to capture an accurate profile, as Auer and Lowrie [7], Stein and Nordlund [9], etc., have noted in other contexts. It also shows that the convergence process is very fast to a fairly accurate solution. However, increasing the number of bins to 1000 does not result in substantial improvement. This is presumably due to a strong frequency dependence of the source and opacity within a bin at points for which the radiation is far from equilibrium. Such a situation causes the approximation (4) to be of poor accuracy.

In Fig. 4 (right), we plot a dimensionless form of the intensity, $(I - I^{\min}_{\text{exact}})/(I^{\max}_{\text{exact}} - I^{\min}_{\text{exact}})$, and compare this quantity for solutions using a small number of bins/bands with those using a large number. For the multigroup case, it can be seen that the 10,000-band solution reaches an acceptable accuracy, whereas the 100,000-band solution is almost exact. This confirms that a high number of bands is required for accurate results. We also see that the 100,000-band method gives accuracy comparable to the 100 bin method and that the 100,000-band method has reached near equivalence to results using all 1.09×10^7 frequencies. If one can afford a large number of frequency subintervals (bins or bands) $\gg 5000$, we recommend the use of the multigroup methods due to their simplicity. However, if one wants to use $\lesssim 100$ frequency subintervals, we recommend the use of the multibin methods. In our case, we have demonstrated that the 10-bin solution achieves a reasonable accuracy. We believe that

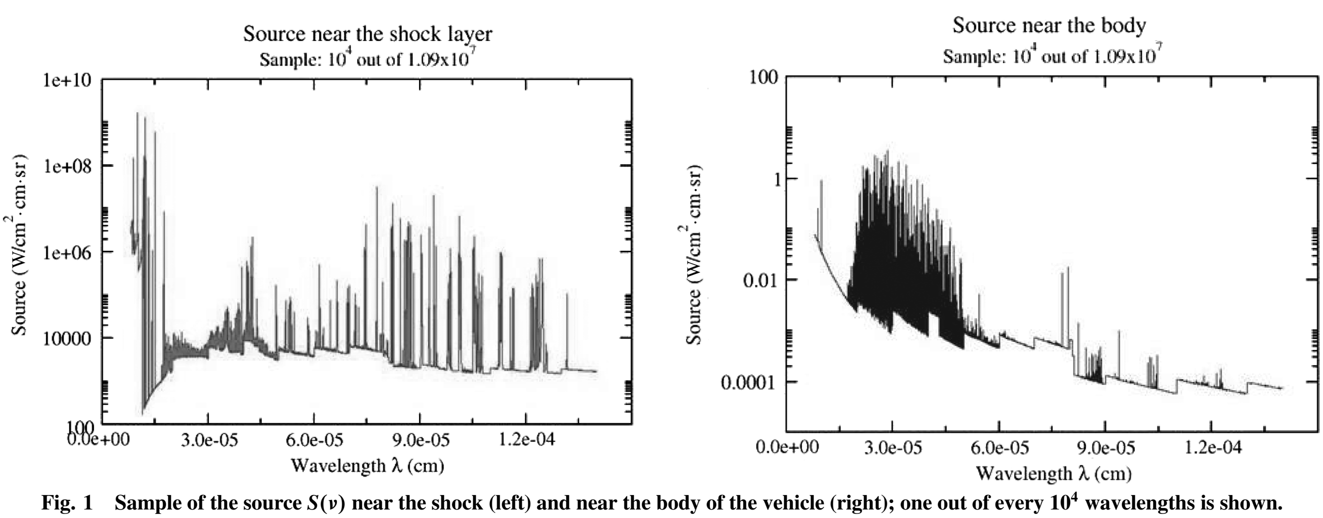

Fig. 1 Sample of the source $S(\nu)$ near the shock (left) and near the body of the vehicle (right); one out of every 10^4 wavelengths is shown.

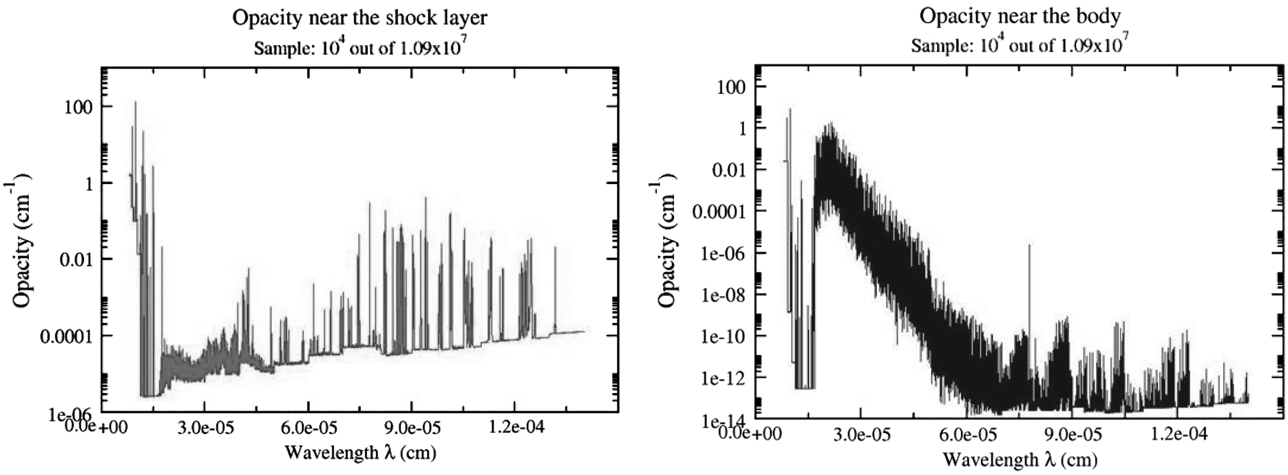

Fig. 2 Sample of the opacity $\sigma(\nu)$ near the shock (left) and near the body of the vehicle (right); one out of every 10^4 wavelengths is shown.

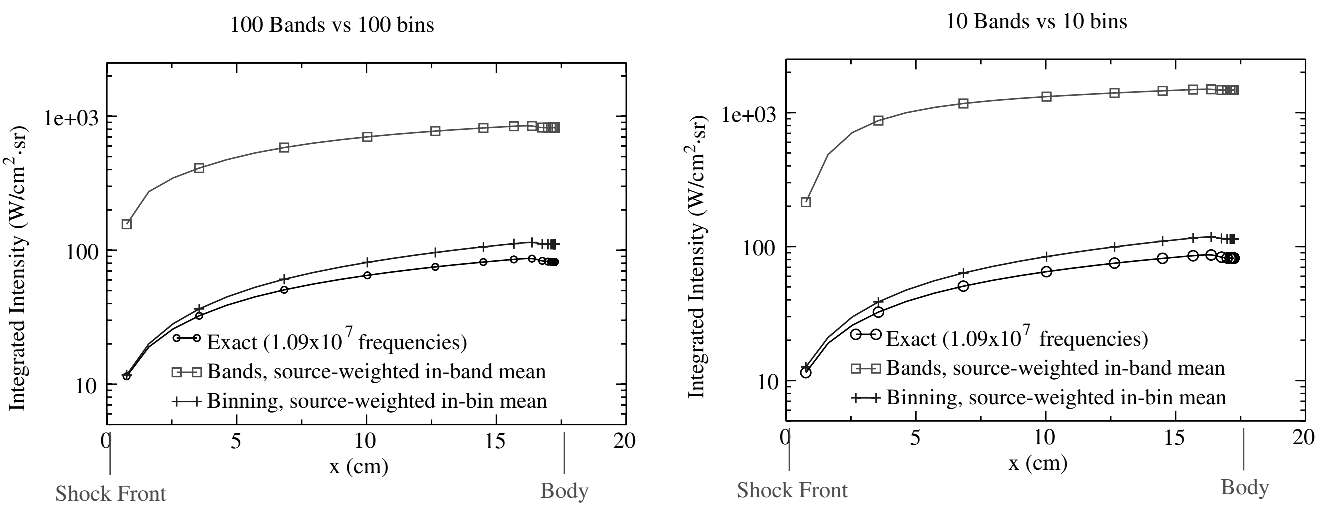

Fig. 3 Comparison of the radiative intensity computed with $n_g = n_b = 100$ (left) and with $n_g = n_b = 10$ (right).

the accuracy of the multibin method could be improved if the local opacity was used to define the bins. This would lessen the chance that some spatial points would have high variability with frequency within a bin, but leads to noncommutivity between the spatial derivative and the bin integral in the integrated RTE.

In Fig. 4 (left), we can see that close to the body, the opacity deviates strongly from the global-mean-based bin values, toward lower values. For bins lower than five, this should have no impact on the accuracy of the bin solution, because the opacity of these bins is already very low (less than 10^{-3} cm^{-1}). Similarly, the values of the

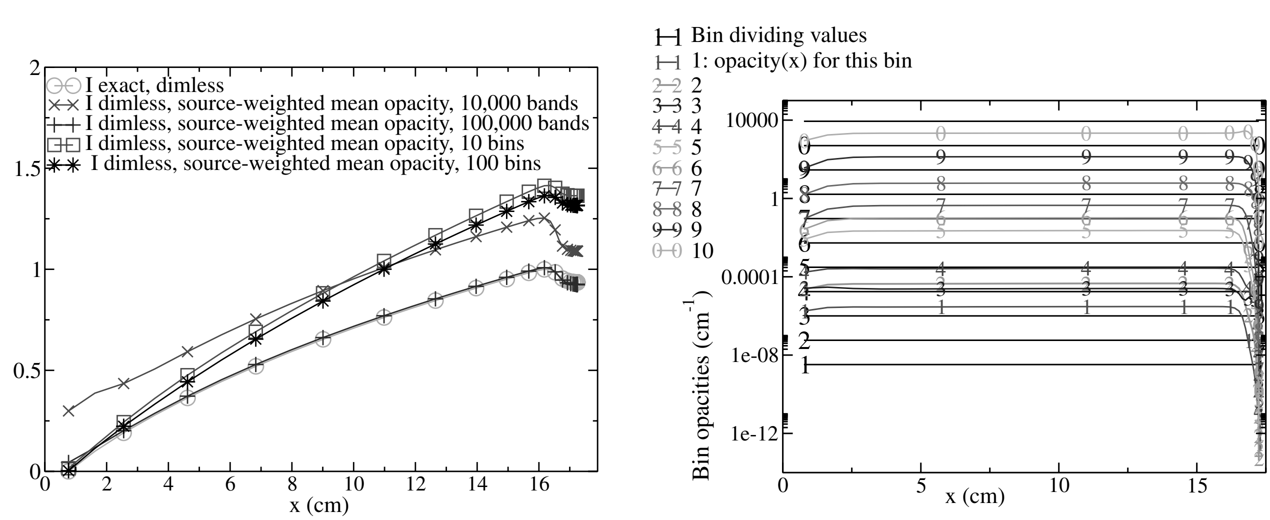

Fig. 4 Dimensionless intensities compared for different bin and group numbers (left) and source-weighted opacities and bin opacity boundaries (right), where the 10th bin is denoted as zero.

local opacities of those bins deviate by one or two bins from their respective global-mean-based bin values on most of the domain ($0 < x < 16$). But because the 10-bin solution is overall quite accurate in this domain, we conclude that this deviation does not have a strong impact. Again, this is due to the very low opacities of those bins (less than 10^{-3} cm^{-1}). However, if the semi-opaque and opaque bins have local transparent opacities, which happens for bins 6 to 10 close to the body, then an important loss of accuracy occurs. This explains why the accuracy of the multibin method is lower close to the body.

V. Conclusions

We demonstrated that the radiation problem of the Apollo AS-501 reentry can be solved accurately by discretizing the RTE into 10 opacity bins, instead of using the full set of $\sim 10^7$ frequencies. This leads to a huge reduction in numerical cost in the RTE solution. In addition, we have shown that it is not possible to obtain such a high accuracy by using a small number of frequency groups. In fact, 10,000 groups are needed to obtain the same order of accuracy as the 10-bin solution. We have thus confirmed that the ODF method is effective for the radiative transfer problem in hypersonic reentry. However, if one could afford a number larger to 10,000 groups, we recommend the use of the multigroup method.

Both the multibin and multigroup methods obviously converge to the exact solution as the number of bins/groups approaches the total number of resolved frequency points, with the slight caveat for binning that if two or more frequencies have exactly the same opacity, so that they fall in the same bin no matter how many bins are used, then the individual intensities for those frequencies can never be separately computed. But the point of the current work is to construct a method that allows accurate answers with a very small frequency-space sampling (10 or 20). This is to allow fully coupled radiation-hydrodynamics simulations of reentry to be affordable on current computers. As just noted, the multibin method seems to satisfy this need, though checking with other reentry data sets must certainly be done. Finally, it should be noted that the computation of the mean opacities (3) and of the bin-total source still form the dominant computational cost.

Acknowledgments

The second author's work was funded by the U.S. Department of Energy and National Nuclear Security Agency. We thank S. Moreau for fruitful discussions on NEQAIR96 [11].

References

[1] Whiting, E. E., Park, C., Liu, Y., and Arnold, J. O., and Paterson, J. A., "NEQAIR96, Nonequilibrium and Equilibrium Radiative Transport and Spectra Program: User Manual," NASA RP-1389, 1996.

[2] Mihalas, D., and Mihalas, B., *Foundations of Radiation Hydrodynamics*, Dover, New York, 1999.

[3] Strom, S. E., and Kurucz, R. L., "A Statistical Procedure For Computing the Line-Blanketed Model Stellar Atmosphere with Applications to the F5 IV Star Procyon," *Journal of Quantitative Spectroscopy and Radiative Transfer*, Vol. 6, No. 1, 1966, pp. 59–147.

[4] Kurucz, R. L., "Model Atmospheres for G, F, A, B, and O Stars," *Astrophysical Journal Supplement Series*, Vol. 40, No. 1, 1979, pp. 1–340.

[5] Nordlund, A., "Numerical Simulations of the Solar Granulation, 1: Basic Equations and Methods," *Astronomy and Astrophysics*, Vol. 102, No. 1, 1982, pp. 1–10.

[6] Mihalas, D., and Auer, L. H., "On Laboratory-Frame Radiation Hydrodynamics," *Journal of Quantitative Spectroscopy and Radiative Transfer*, Vol. 71, No. 1, Oct. 2001, pp. 61–97.

[7] Auer, L. H., and Lowrie, R. B., "Dispersion Analysis of Radiation/Thermal Fronts With Fully Resolved Spectral Opacity Variation," Los Alamos National Lab., Rept. LA-UR-00-6094, Los Alamos, NM, 2000.

[8] Cullen, D. E., and Pomraning, G. C., "The Multiband Method in Radiative Transfer Calculations," *Journal of Quantitative Spectroscopy and Radiative Transfer*, Vol. 24, Aug. 1980, pp. 97–117.

[9] Stein, R. F., and Nordlund, A., "Realistic Solar Convection Simulations," *Solar Physics*, Vol. 192, Nos. 1–2, 2000, pp. 91–108.

[10] Ripoll, J.-F., Dubroca, B., and Duffa, G., "Modelling Radiative Mean Absorption Coefficients," *Combustion Theory and Modeling*, Vol. 5, No. 3, 2001, pp. 261–275.

[11] Moreau, S., "Computation of High Altitude Hypersonic Flow-Field Radiation," Ph.D. Thesis, Stanford Univ., Stanford, CA, 1993.

[12] Wright, M. J., Candler, G., and Bose, D., "Data-Parallel Line Relaxation Method for the Navier-Stokes Equations," *AIAA Journal*, Vol. 36, No. 9, 1998, pp. 1603–1609.

[13] Wright, M. J., Prabhu, D. K., and Martinez, E. R., "Analysis of Afterbody Heating Rates on the Apollo Command Modules, Part 1: AS-202," *Journal of Thermophysics and Heat Transfer*, Vol. 20, No. 1, 2006, pp. 16–30.

J. Gore
Associate Editor